permitted. Finally, we enrolled 24 patients with sinus rhythm and blood pressure-preserved "wet and cold" heart failure. We did not use the intravenous infusion of digitalis, and none of the patients in the present study were taking oral digitalis. Before the initiation of treatment, all patients underwent blood sampling, and an electrocardiogram, echocardiogram, and chest x-rays.

Measurement of blood pressure and heart rate: Blood pressure monitoring was performed using the TaskForce Monitor 3040i (CNSystems, Austria). The cuff was attached to a finger on the left hand and supported at heart level. Electrocardiogram electrodes were attached to the chest. Once a reading of blood pressure and heart rate had stabilized, 3 consecutive 5-minute recordings were made of the blood pressure and electrocardiogram tracing. Noninvasive brachial blood pressure readings were taken with an appropriate sized cuff.

Measurement of BRS by spontaneous sequence method: Sequence analysis detected sequences of 3 or more beats in which there was either an increase in SBP and pulse interval (Up sequence) or a decrease in SBP and pulse interval (Down sequence). The sequences involving premature ventricular contraction were excluded. BRS was estimated as the mean slope of the up sequences (Up BRS), the down sequences (Down BRS), and also the mean slope of all sequences (Sequence BRS).[14,15] Previous reports showed that this protocol measures BRS accurately in animals compared with standard pharmacological techniques.[14-16]

MIL responders and nonresponders: Blood sampling was performed in all patients, and the severity of tricuspid regurgitation (TR) was evaluated by color-flow Doppler (graded as trivial, mild, moderate, or severe). TR pressure gradient (TRPG) was measured by echocardiography and BRS was measured by the spontaneous sequence method before and 2 hours after the initiation of intravenous infusion of milrinone (0.25 μg/kg/minute). We did not do an initial bolus infusion. The effects of MIL are reported to be stable and plateau at 2 hours after the initiation of MIL.[18] At 2 hours after administration, milrinone improved dyspnea, urine volume (> 100 mL/hour), and the severity of tricuspid regurgitation in 13 patients (responders; R), whereas no improvement was observed in 11 patients (nonresponders; NR) (Figure 1). The degree of dyspnea was assessed by the modified Borg scale.[19] An improvement in dyspnea was defined as a reduction of 2 or more in the modified Borg scale score.[20]

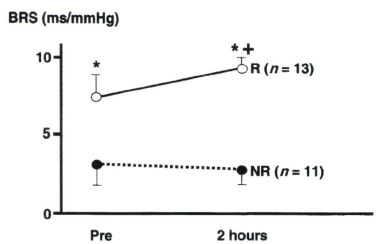

Figure 1. Baseline BRS was significantly lower in the NR group than in the R group. At 2 hours after milrinone treatment, BRS was also significantly lower in the NR than in the R group. Furthermore, in the R group, BRS at 2 hours was significantly higher than that at baseline. *$P < 0.05$ versus NR group. +$P < 0.05$ versus pre.

Statistical analysis: Normally distributed variables are expressed as the mean ± SD. The unpaired t test or Mann-Whitney U test was used to compare the differences in normally distributed variables, respectively, between the R group and NR group. All statistical tests were carried out against the baseline characteristics. Differences were considered significant at a P value of < 0.05. A receiver operating characteristic (ROC) curve was used to determine the discriminatory ability of BRS on the occurrence of response to MIL. An ROC-curve (plot of sensitivity versus 1-specificity) analysis is a powerful tool for assessing a test's ability to discriminate between R and NR groups of subjects.

Results

Patient characteristics at baseline: The patient profiles at enrollment are summarized in Tables I and II. As can be seen in Table I, there were no significant differences in age, gender, or the prevalence of dilated cardiomyopathy, hypertensive heart disease, or valvular heart disease between the R and NR group just before the milrinone therapy. Prior medications were not different either.

As shown in Table II, hemoglobin, brain natriuretic peptide (BNP) measured at discharge, and the estimated glomerular filtration rate (eGFR) did not differ between the two groups. Left ventricular ejection fraction (LVEF), left ventricular end-diastolic dimension (LVEDD), left ventricular end-systolic dimension (LVESD), and TRPG assessed by echocardiography

Table I. Baseline Characteristics

	R	NR	P
n	13	11	
Male	8	7	NS
Age	58 ± 7	59 ± 5	NS
BMI	22 ± 4	23 ± 3	NS
Body weight (kg)	56 ± 7	53 ± 9	NS
Current smoker	4 (31%)	3 (27%)	NS
Causes of heart failure			
Coronary artery disease	4 (31%)	4 (36%)	NS
Dilated cardiomyopathy	4 (31%)	3 (27%)	NS
Hypertensive heart disease	3 (23%)	2 (18%)	NS
Valvular heart disease	2 (15%)	2 (18%)	NS
NYHA functional classification			
III	9 (69%)	8 (73%)	NS
IV	4 (31%)	3 (27%)	NS
Modified Borg scale	6.1 ± 1.8	6.4 ± 2.2	NS
Systolic blood pressure (mmHg)	118 ± 11	121 ± 14	NS
Diastolic blood pressure (mmHg)	78 ± 14	73 ± 9	NS
Heart rate (bpm)	108 ± 9	111 ± 13	NS
Medications			
Diuretics	7 (54%)	6 (55%)	NS
β-Blockers	9 (69%)	8 (73%)	NS
ACE inhibitors	10 (77%)	8 (73%)	NS
Angiotensin receptor blocker	3 (23%)	3 (27%)	NS

Data are presented as number (%) or mean ± SD. BMI indicates body mass index; NYHA, New York Heart Association; and NS, not significant.

Table II. Baseline Characteristics (2)

	R (n = 13)	NR (n = 11)	P
Total cholesterol (mg/dL)	187 ± 33	172 ± 44	NS
LDL cholesterol (mg/dL)	94 ± 31	102 ± 43	NS
HDL cholesterol (mg/dL)	42 ± 8	45 ± 7	NS
Triglycerides (mg/dL)	119 ± 27	120 ± 31	NS
Hemoglobin (g/dL)	9.8 ± 1.4	10.3 ± 2.1	NS
Hematocrit (%)	35 ± 3	34 ± 3	NS
Total bilirubin (mg/dL)	1.3 ± 0.2	1.4 ± 0.3	NS
AST/ALT (U/L)	47 ± 4 / 36 ± 8	57 ± 4 / 45 ± 6	< 0.05 / < 0.05
Serum sodium (mmol/L)	131 ± 3	132 ± 2	NS
FBS (mg/dL)	82 ± 17	99 ± 15	NS
HbA1c (%)	5.2 ± 0.7	5.3 ± 0.4	NS
BNP (pg/mL)	188 ± 27	194 ± 36	NS
eGFR (mL/minute/1.73m^2)	61.4 ± 7.9	62.8 ± 4.9	NS
LVEF (%)	37 ± 7	34 ± 5	NS
LVEDD (mm)	58 ± 6	59 ± 7	NS
LVESD (mm)	42 ± 4	43 ± 7	NS
IVC (mm)	18 ± 4	24 ± 3	< 0.05
TRPG (mmHg)	47 ± 8	51 ± 9	NS
BRS (ms/mmHg)	7.3 ± 1.2	3.2 ± 1.6	< 0.05

Data are presented as number (%) or mean ± SD. LDL indicates low-density lioprotein; HDL, high-density lipoprotein; HbA1c, hemoglobin A1c; eGFR, creatinine-based estimate of glomerular filtration rate; LVEF, left ventricular ejection fraction; LVEDD, left ventricular end-diastolic dimension; LVESD, left ventricular end-systolic dimension; TRPG, tricuspid regurgitant pressure gradient; BRS, baroreflex sensitivity; and NS, not significant.

Table III. Effects of Milrinone at 2 Hours

	R (n = 13)	NR (n = 11)	P
Modified Borg scale	3.3 ± 1.6	6.2 ± 1.9	< 0.05
TRPG (mmHg)	29 ± 4	49 ± 7	< 0.05
Urine volume (mL/hour)	128 ± 18	42 ± 23	< 0.05
SBP (mmHg)	106 ± 15	114 ± 18	NS
Serum sodium level (mmol/L)	135 ± 2	129 ± 3	< 0.05
LVEF (%)	42 ± 3	36 ± 2	< 0.05
HR (bpm)	82 ± 15	106 ± 12	< 0.05

Data are presented as number (%) or mean ± SD. TRPG indicates tricuspid regurgitant pressure gradient; SBP, systolic blood pressure; LVEF, left ventricular ejection fraction; and HR, heart rate.

were not different between the two groups. AST and inferior vena cava diameter were significantly higher in the NR group than in the R group. Median BRS was significantly higher in the R group than in NR prior to the milrinone infusion (7.3 ± 1.2 versus 3.211.6 ms/mmHg, $P < 0.05$).

Effects of MIL at 2 hours: In the R group, the modified Borg scale score and TRPG at 2 hours were significantly lower than in the NR group (Table III). Urine volume per hour at 2 hours was over 100 mL/hour in all patients in the R group and significantly higher than in the NR group (Table III). LVEF and the serum sodium level were significantly higher in the R group than in the NR group (Table III). Systolic blood pressure at 2 hours was not changed. However, heart rate at 2 hours was significantly lower in the R group than in the NR group (Table III).

BRS at 2 hours: At 2 hours after the milrinone infusion, BRS was further increased in the R group, whereas it failed to increase in the NR group (Figure 1). The sensitivity and specificity for BRS at a cut-off level of 5 ms/mmHg were 0.94 and 0.93, respectively. The negative and positive predictive values were 0.98 and 0.71 (Figure 2).

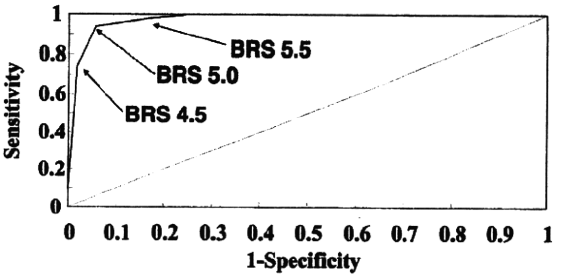

Figure 2. Receiver operator curve of BRS for prediction of responders to milrinone.

Discussion

In the present study, we demonstrated that baroreflex sensitivity measured by a spontaneous sequence method was significantly lower in the nonresponder group to milrinone than in the responder group to milrinone in patients with sinus rhythm and blood pressure-preserved "wet and cold" heart failure. Furthermore, the sensitivity and specificity for BRS at a cut-off level of 5 ms/mmHg was 0.94 and 0.93. These results suggested that BRS might be clinically useful for the prediction of responders to milrinone among patients with sinus rhythm and blood pressure-preserved "wet and cold" heart failure.

Milrinone is recommended for patients with "wet and cold" heart failure,[2] which is determined as heart failure with congestion and hypoperfusion.[3] In cases in which the systolic blood pressure is under 100 mmHg, the combination of milrinone and dobutamine is necessary.[1] However, among patients with "wet and cold" heart failure whose systolic blood pressure is over 100 mmHg, milrinone monotherapy is often insufficient. In the present study, 11 of 24 patients with "wet and cold" heart failure whose systolic blood pressure was over 100 mmHg were nonresponders to milrinone. Based on these results, we believe that systolic blood pressure is not clinically useful for predicting the response to milrinone. This is the first study to demonstrate the cut-off levels of parameters for predicting the response to milrinone, and BRS assessed by a spontaneous sequence method might be a new and novel therapeutic parameter.

A sustained baroreflex-mediated increase in sympathetic activity may contribute to increased end-organ damage and to progression of the underlying disease, and a blunted baroreflex gain is predictive of increased cardiovascular risk in postmyocardial infarction and heart failure patients.[7] Recently, the prognostic value of BRS obtained noninvasively by the modified transfer function method has been assessed in a cohort of 317 mild-to-moderate clinically stable heart failure patients. In 55 of the 228 subjects with a measurable index, a depressed BRS (≤ 3.1 ms/mmHg) was significantly associated with a higher risk of cardiac death. The results of the present study are compatible with a previous study.[16] We believe that BRS might be clinically useful as a parameter with which to determine the severity of heart failure.

The spontaneous sequence method is a noninvasive and easy method for measuring BRS in patients with acute heart failure. The advantages of this method are twofold: (i) computations are automatic and standardized, which virtually eliminates intra- and intersubject measurement variability, and (ii) distinct measurements are obtained for increasing and decreasing arterial pressure values, thus allowing one to take into account the well-known asymmetry of the baroreceptor response.[7] Further studies are necessary to determine whether other noninvasive methods to measure BRS are clinically useful or not.

The mechanisms in which BRS predicts the responses to milrinone were not fully determined in the present study. Previous studies have suggested that arterial baroreflex control of HR is diminished in heart failure,[11,21] and that the contribution of baroreflex control in myocardial contractility is markedly impaired in animals with a lower baseline inotropic state.[22] Furthermore, in heart failure, baroreflex changes in cardiac output are less related to changes in HR and more related to changes in stroke volume.[23] Milrinone is considered to exert a positive inotropic action and to decrease left ventricular end-systolic pressure reflecting the decrease in left ventricular afterload.[24] However, milrinone-induced reductions in effective arterial elastance reflecting the fall in total peripheral resistance and changes in stroke volume are not significant.[24] These previous reports suggested that baroreflex control is important to obtain the inotropic effect of milrinone. Another previous study suggested that BRS predicts the cases in which milrinone increases left ventricular *dp/dt*.[4] The increase in left ventricular *dp/dt* indicates milrinone has an inotropic effect. In the present study, in the R group, the treatment with milrinone for 2 hours was considered to increase cardiac output because LVEF and serum sodium levels were significantly increased. Moreover, AST and inferior vena cava diameter were significantly higher in the NR group than in the R group. These results suggest that right ventricular function was impaired in the NR group to a greater extent than in the R group. Nonresponders to milrinone can be considered to be a higher severity group of heart failure than responders to milrinone. However, we did not have the direct data of cardiac output, chest x-rays, and electrocardiogram in the present study. Further studies monitoring hemodynamic parameters (involving cardiac output) of the patients with acute heart failure treated with milrinone are necessary.

There are several limitations to the present study. First, it is a small and retrospective study. It is necessary to examine the predictive value of BRS in a large-scale population in which the distribution of BRS is normal. Second, we excluded patients with atrial fibrillation. In patients with atrial fibrillation, the spontaneous sequence method is not feasible. However, among patients with acute heart failure, there are many patients with atrial fibrillation. We believe that BRS measured by the spontaneous sequence method can only be used in patients with sinus rhythm. Third, we examined the effects of milrinone for only 2 hours. Furthermore, the present study is retrospective. Fourth, we did not perform the hemodynamic assessment using a Swan-Ganz catheter, and we defined low cardiac output from the clinical state of "cold and wet". There were no variables to show the fact by echocardiography or Swan-Ganz catheter. Randomized study with the assessment of hemodynamic data obtained by Swan-Ganz catheter should be performed.

Conclusions: The results of the present study suggested that baroreflex sensitivity to milrinone measured by the spontaneous sequence method was significantly lower in the nonresponder group than in the responder group in patients with "wet and cold" heart failure and that the cut-off level of BRS is 5 ms/mmHg. We believe that BRS might be clinically useful for the prediction of responders to milrinone in patients with "wet and cold" heart failure.

Acknowledgments

We are grateful to the staff of the Department of Cardiovascular Medicine of Kyushu University Graduate School of Medical Sciences. Furthermore, we wish to thank Dr. Kazuhisa Kodama, the chair of the Nakanoshima Heart Failure Conference.

References

1. Task Force for Diagnosis and Treatment of Acute and Chronic Heart Failure 2008 of European Society of Cardiology, Dickstein K, Cohen-Solal A, *et al.* ESC Guidelines for the diagnosis and treatment of acute and chronic heart failure 2008: the Task Force for the Diagnosis and Treatment of Acute and Chronic Heart Failure 2008 of the European Society of Cardiology. Developed in collaboration with the Heart Failure Association of the ESC (HFA) and endorsed by the European Society of Intensive Care Medicine (ESICM). Eur Heart J 2008; 29: 2388-442. (Review)
2. Shin DD, Brandimarte F, DeLuca L, *et al.* Review of current and investigational pharmacologic agents for acute heart failure syndromes. Am J Cardiol 2007; 99: 4A-23A. (Review)
3. Nohria A, Tsang SW, Fang JC, *et al.* Clinical assessment identifies hemodynamic profiles that predict outcomes in patients admitted with heart failure. J Am Coll Cardiol 2003; 41: 1797-804.
4. Sato N, Yamamoto T, Akutsu K, *et al.* Arterial baroreflex sensitivity is a good predictor of inotropic responses to a phosphodiesterase inhibitor in human heart failure. Clin Cardiol 2006; 29: 263-7.
5. Cowley AW Jr, Liard JF, Guyton AC. Role of baroreceptor reflex in daily control of arterial blood pressure and other variables in dogs. Circ Res 1973; 32: 564-76.
6. Mancia G, Grassi G, Bertinieri G, Ferrari A, Zanchetti A. Arterial baroreceptor control of blood pressure in man. J Auton Nerv Syst 1984; 11: 115-24. (Review)
7. La Rovere MT, Pinna GD, Raczak G. Baroreflex sensitivity: measurement and clinical implications. Ann Noninvasive Electrocardiol 2008; 13: 191-207. (Review)
8. Latinen T, Hartikainen J, Vanninen E, Niskanen L, Geelen G, Länsimies E. Age and gender dependency of baroreflex sensitivity in healthy subjects. J Appl Physiol 1998; 84: 576-83.
9. Farrell TG, Odemuyiwa O, Bashir Y, *et al.* Prognostic value of baroreflex sensitivity testing after acute myocardial infarction. Br Heart J 1992; 67: 129-37.
10. La Rovere MT, Bigger JT Jr, Marcus FI, Mortara A, Schwartz PJ. Baroreflex sensitivity and heart-rate variability in prediction of total cardiac mortality after myocardial infarction. ATRAMI (Autonomic Tone and Reflexes After Myocardial Infarction) Investigators. Lancet 1998; 351: 478-84.
11. Mortara A, La Rovere MT, Pinna GD, *et al.* Arterial baroreflex modulation of heart rate in chronic heart failure: clinical and hemodynamic correlates and prognostic implications. Circulation 1997; 96: 3450-8.
12. Imholz BP, Wieling W, Langewouters GJ, van Montfrans GA. Continuous finger arterial pressure: utility in the cardiovascular laboratory. Clin Auton Res 1991; 1: 43-53.
13. Imholz BP, Wieling W, van Montfrans GA, Wesseling KH. Fifteen years experience with finger arterial pressure monitoring: assess-

ment of the technology. Cardiovasc Res 1998; 38: 605-16. (Review)
14. Waki H, Kasparov S, Wong LF, Murphy D, Shimizu T, Paton JF. Chronic inhibition of endothelial nitric oxide synthase activity in nucleus tractus solitarii enhances baroreceptor reflex in conscious rats. J Physiol 2003; 546: 233-42.
15. Waki H, Katahira K, Polson JW, Kasparov S, Murphy D, Paton JF. Automation of analysis of cardiovascular autonomic function from chronic measurements of arterial pressure in conscious rats. Exp Physiol 2006; 91: 201-13.
16. Pinna GD, Maestri R, Capomolla S, *et al.* Applicability and clinical relevance of the transfer function method in the assessment of baroreflex sensitivity in heart failure patients. J Am Coll Cardiol 2005; 46: 1314-21.
17. Eriksson H, Svärdsudd K, Larsson B, *et al.* Risk factors for heart failure in the general population: the study of men born in 1913. Eur Heart J 1989; 10: 647-56.
18. Nolan J, Sanderson A, Taddei F, Smith S, Muir AL. Acute effects of intravenous phosphodiesterase inhibition in chronic heart failure: simultaneous pre- and afterload reduction with a single agent. Int J Cardiol 1992; 35: 343-9.
19. Borg G. Psychophysical bases of perceived exertion. Med Sci Sports Exerc 1982; 14: 377-81.
20. Nomura F, Kurobe N, Mori Y, *et al.* Multicenter prospective investigation on efficacy and safety of carperitide as a first-line drug for acute heart failure syndrome with preserved blood pressure: COMPASS: Carperitide Effects Observed Through Monitoring Dyspnea in Acute Decompensated Heart Failure Study. Circ J 2008; 72: 1777-86.
21. Floras JS. Sympathetic nervous system activation in human heart failure: clinical implications of an updated model. J Am Coll Cardiol 2009; 54: 375-85. (Review)
22. Jung AS, Harrison R, Lee KH, *et al.* Simulated microgravity produces attenuated baroreflex-mediated pressor, chronotropic, and inotropic responses in mice. Am J Physiol Heart Circ Physiol 2005; 289: H600-7.
23. Sala-Mercado JA, Ichinose M, Hammond RL, *et al.* Spontaneous baroreflex control of heart rate versus cardiac output: altered coupling in heart failure. Am J Physiol Heart Circ Physiol 2008; 294: H1304-9.
24. Kishi T, Nakahashi K, Ito H, Taniguchi S, Takaki M. Effects of milrinone on left ventricular end-systolic pressure-volume relationship of rat hearts in situ. Clin Exp Pharmacol Physiol 2001; 28: 737-42.

32nd Annual International Conference of the IEEE EMBS
Buenos Aires, Argentina, August 31 - September 4, 2010

Development of artificial bionic baroreflex system

Kenji Sunagawa, *Senior Member, IEEE* and Masaru Sugimachi, *Member, IEEE*

***Abstract*—The baroreflex system is the fastest mechanism in the body to regulate arterial pressure. Because the neural system (i.e., autonomic nervous system) mediates the baroreflex and the system operates under the closed-loop condition, the quantitative dynamic characteristics of the baroreflex system remained unknown until recently despite the fact that a countless number of observational and qualitative studies had been conducted. In order to develop the artificial baroreflex system, i.e., the bionic baroreflex system, we first anatomically isolated the carotid sinuses to open the baroreflex loop and identified the open-loop transfer function of the baroreflex system using white noise pressure perturbations. We found that the baroreflex system is basically a lowpass filter and remarkably linear. As an actuator to implement the bionic baroreflex system, we then stimulated the sympathetic efferent nerves at various parts of the baroreflex loop and identified the transfer functions from the stimulation sites to systemic arterial pressure. We found that the actuator responses can be described remarkably well with linear transfer functions. Since transfer functions of the native baroreflex and of the actuator were identified, the controller that is required to reproduce the native baroreflex transfer function can be easily derived from those transfer functions. To examine the performance of bionic baroreflex system, we implemented it animal models of baroreflex failure. The bionic baroreflex system restored normal arterial pressure regulation against orthostatic stresses that is indistinguishable from the native baroreflex system.**

I. Introduction

Baroreflex is known to be the fastest mechanism in the body to stabilize arterial pressure. The reflex makes use of negative feedback mechanism. The baroreceptors sitting in the arterial wall sense arterial pressure and send the pressure signal to the brainstem through the afferent nerve fibers. The brainstem receives the pressure signal and judges the level of arterial pressure. If the level is low, the brainstem activates the sympathetic system innervating the heart and vascular system to increase arterial pressure. If the level of arterial pressure is high, the brainstem withdraws the sympathetic activation.

The baroreflex system is critically important in animal, particularly in human. This is because, unlike animals with four legs, the position dependent gravitational effect on circulation is most prominent in human. It is well known that once we lose the normal function of baroreflex, we no longer keep sitting and/or standing positions because of position induced profound hypotension and hypoperfusion of the brain. Baroreflex failure destroys normal life and is a devastating pathological state in human. However, since the baroreflex failure is a disease of the neural system, no effective treatment has ever developed to save those patients.

Baroreflex failure could happen under various conditions. In some patients, they lost baroreflex function because they have problems in the baroreceptors, the brainstem and/or the spinal cord. In those patients, if we can develop a mechanism to activate their sympathetic efferent system in response to changes in arterial pressure just like the native brainstem does, in theory, normal baroreflex function can be restored.

The purpose of this investigation is to develop an artificial baroreflex system, so called the bionic baroreflex system, to restore normal baroreflex function to overcome such a serious pathological condition.

II. Bionic Baroreflex System

Shown in Fig. 1 are how we identify the transfer function of the controller of bionic baroreflex system. First we identify the transfer function of the baroreflex open loop (H_{NATIVE}) from baroreceptor pressure to arterial pressure responses. We then electrically stimulate a particular site in the baroreflex loop and identify the transfer function of the actuator from the stimulation to arterial pressure responses ($H_{STM \rightarrow AOP}$). Since the controller will be in series with the actuator, the transfer function of bionic baroreflex system becomes identical to the native baroreflex system when the transfer function of controller (H_{BIONIC}) satisfies the following equation:

$$H_{NATIVE} = H_{BIONIC} \times H_{STM \rightarrow AOP}$$

In theory both H_{NATIVE} and $H_{STM \rightarrow AOP}$ can be experimentally determined. Therefore, H_{BIONIC} can be determined. However whether such a simple approach works or not highly depends on the simplicity of the native baroreflex system including the system linearity. We therefore examined the dynamic characteristics of baroreflex system.

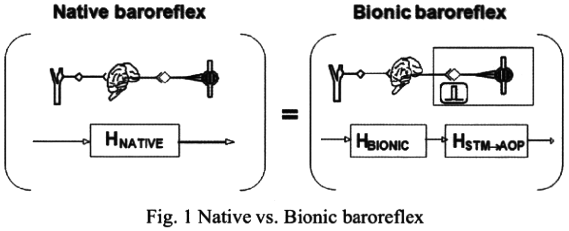

Fig. 1 Native vs. Bionic baroreflex

We vascularily isolated the baroreceptors (carotid sinuses) in rats (n=10) to open the baroreflex feedback loop and connected the carotid sinuses to a servo-controlled piston pump. This preparation allowed us to manipulate the carotid sinus pressure (CSP) independent of arterial pressure. We then perturbed CSP with random binary pressure sequences and identified the transfer function from CSP to arterial pressure. Shown in the left panels of Fig. 2 are the time series of CSP and aortic pressure. As can be seen, aortic pressure changes slowly toward the opposite direction in response to changes in CSP. This becomes even more evident in the transfer function (the right panel). The transfer function has low-pass filter characteristics. The phase response becomes nearly out-of-phase in the low frequency range suggesting the negative feedback nature of baroreflex system. Note that the magnitude squared coherence function is about 0.8 over the frequency range of interest. This is to say that most dominant characteristics of the total baroreflex open loop are captured by the linear transfer function.

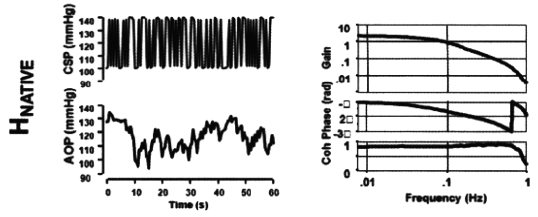

Fig. 2 Dynamic characteristics of native baroreflex system

In order to identify the actuator transfer function, we electrically stimulated the celiac ganglia with random binary pressure perturbations. Illustrated in the left panels of Fig. 3 are the time series of stimulation of celiac ganglia and aortic pressure responses. As can be seen, aortic pressure changes slowly toward the same direction in response to changes in stimulation. As anticipated the transfer function (the right panel) has low-pass filter characteristics. Unlike the total baroreflex loop, however, the phase response becomes nearly in-phase in the low frequency range. The magnitude squared coherence function is about 0.8 over the frequency range of interest. Again, it is reasonable to assume that most dominant characteristics of the actuator are captured by the linear transfer function.

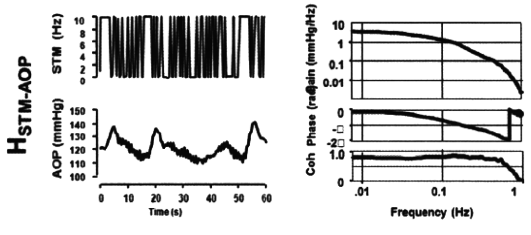

Fig. 3 Dynamic characteristics of sympathetic stimulation

We identified the transfer function (H_{BIONIC}) required for the controller by taking the ratio of H_{NATIVE} to $H_{STM \rightarrow AOP}$. Since both dynamic characteristics of the total baroreflex loop and actuator are well represented by the linear transfer functions, the resultant H_{BIONIC} should reproduce the native characteristics of the baroreflex system when the feedback loop is closed. Shown in Fig. 4 are the changes in arterial pressure in response to orthostatic stresses under the open-loop baroreflex condition (baroreflex failure), the closed-loop baroreflex condition (native baroreflex) and the bionic baroreflex condition. Orthostatic stresses profoundly lowered arterial pressure in the absence of the native baroreflex. Closing the native baroreflex loop markedly attenuated the hypotensive responses. The activation of bionic baroreflex system also attenuated the hypotensive response as much as the native baroreflex system did. Statistical analysis indicated that the pressure regulation achieved by the bionic baroreflex system was indistinguishable from that achieved by the native baroreflex system.

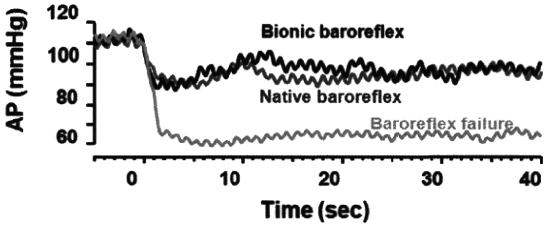

Fig. 4 Native baroreflex system vs. bionic baroreflex system

III. Discussion

We have shown that the bionic baroreflex system was as good as the native baroreflex system in regulating arterial pressure. The dynamic pressure responses to orthostatic stresses were indistinguishable between the native baroreflex system and the bionic baroreflex system. Although the baroreflex system is known to be nonlinear over the wide pressure range, we found that it is remarkably linear in the physiological pressure range. Because of this, the linear transfer function could represent the dominant characteristics of the baroreflex loop, and thereby allowed us to develop the bionic baroreflex system.

We can think of many anatomical sites where we can manipulate the activity of sympathetic system. In 1992, we stimulated the carotid sinus nerve to control the sympathetic system [1]. In 2004, we stimulated the spinal cord to stimulate the sympathetic efferent fibers [2]. The bionic mechanism worked beautifully regardless of the site of stimulation. It equally worked well in rats [3], rabbits [2], and dogs [1]. Although our experience of baroreflex failure in patients is limited, judging from its robustness, the bionic baroreflex system would work in patients as well [4]. If the bionic baroreflex system works in patients, it has a major impact as the treatment of baroreflex failure [5] that has been considered to be an incurable devastating disease.

IV. Conclusion

The bionic baroreflex system restores normal baroreflex function in an animal model of baroreflex failure.

ACKNOWLEDGMENT

This study was supported in part by Health and Labour Sciences Research Grant for Research on Medical Devices for Improving Impaired QOL from the Ministry of Health Labour and Welfare of Japan, Health and Labour Sciences Research Grant for Clinical Research from the Ministry of Health Labour and Welfare of Japan, and Grant-in-Aid for Scientific Research(S) (18100006) from the Japan Society for the Promotion of Science.

REFERENCES

[1] T. Kubota, H. Chishaki, T. Yoshida, K. Sunagawa, A. Takeshita, and Y. Nose, "How to encode arterial pressure into carotid sinus nerve to invoke natural baroreflex," *Am J Physiol* 263: H307-H313, 1992

[2] Y. Yanagiya, T. Sato, T. Kawada, M. Inagaki, T. Tatewaki, C. Zheng, A. Kamiya, H. Takaki, M. Sugimachi, and K. Sunagawa, "Bionic epidural stimulation restores arterial pressure regulation during orthostasis," *J Appl Physiol* 97: 984-990, 2004

[3] T. Sato, T. Kawada, T. Shishido, M. Sugimachi, and K. Sunagawa, "Novel therapeutic strategy against central baroreflex failure: A bionic baroreflex system," *Circulation* 100: 299-304, 1999

[4] F. Yamasaki, T. Ushida, T. Yokoyama, M. Ando, K. Yamasaki, and T. Sato, "Artificial baroreflex: clinical application of a bionic baroreflex system," *Circulation* 113: 634-639, 2008

[5] M. Sugimachi, and K. Sunagawa, "Bionic cardiology: exploration into a wealth of controllable body parts in the cardiovascular system," *IEEE Rev Biomed Eng.* 2: 172-186, 2009.

32nd Annual International Conference of the IEEE EMBS
Buenos Aires, Argentina, August 31 - September 4, 2010

The pressure-volume relationship of the heart: Past, Present and Future

Kenji Sunagawa, *Senior Member, IEEE*

Abstract—**The pressure-volume relationship of the heart was first reported more than a century ago. It was not widely accepted, however, until the mid-1970s. The pressure-volume diagram became a central theme of cardiac mechanics once it was shown to be a good representation of ventricular mechanics. Early in 1980s, the introduction of the ventricular interaction with afterload using effective arterial elastance made it possible to translate ventricular mechanical properties represented by the pressure-volume relationship to the pumping ability of the heart. Furthermore incorporating the framework of ventricular arterial interaction into the classic Guyton's circulatory equilibrium early in 2000s enabled us to express quantitatively how mechanical properties of the ventricles and vascular systems determine the circulatory equilibrium. Successful quantitative descriptions of circulatory equilibrium using the pressure-volume concept would promote basic cardiovascular physiology and accelerate its clinical applications.**

I. PAST (~1980S)

In 1899 Otto Frank published a theoretical paper [1] entitled "Die Grundform des arteriellen Pulses," in which he characterized contractions of the frog ventricle in a pressure-volume (P-V) diagram. It is a schematic expression based on experimental data published in 1895. This schematic diagram is perhaps the first complete P-V diagram ever published on the heart. For various reasons, however, the approach was not well accepted. The marked loading history dependence of the end-systolic P-V relation (ESPVR) that Frank and his followers observed in the frog heart had left physiologists and cardiologists with a strong negative feeling about the use of the P-V diagram for understanding cardiac mechanics.

Our experience with isolated, blood-perfused canine hearts differed markedly from those earlier observations. In the physiological range, the ESPVR appeared to be linear and insensitive to changes in loading conditions. Encouraged by our own simple findings and by similar findings of other investigators, we proposed early in 1970s to scrutinize this relationship as a potential candidate for an index of ventricular contractility [2].

The discovery of the simple characteristics of the ESPVR in the canine heart was not the only attraction of the P-V analysis. We knew this approach would yield a great deal of information about cardiac pump function that is not explicit in the time function of the ventricular pressure and volume. The systolic P-V area [3] as a measure of the total mechanical energy released per ventricular contraction is an entirely new concept that could emerge only from the P-V diagram. Another essential production of this approach is the notion of effective arterial elastance [4] that functionally represents the mechanical properties of the afterload system in terms of P-V relationship. The concept of effective arterial elastance made it possible to couple the ventricle with the afterload on the P-V plane to analyze ventricular-arterial interaction. The qualitative expression of ventricular arterial interaction using the P-V diagram sharpened as well as deepened our understanding of the mechanism how the mechanical properties of the ventricle and arterial system determine stroke volume, thus cardiac output [5].

II. PRESENT (1990-2010)

Although the ventricular arterial interaction was quantitatively expressed by the P-V relationship, it remained unknown how the ventricle determines cardiac output by interacting with the total vascular system. Guyton established that cardiac output is determined as the equilibrium between the venous return curve and cardiac output curve [6]. In 2004 we developed and experimentally validated an algebraic expression of cardiac output curve by extensively using the ventricular arterial P-V relationship. Incorporating the derived cardiac output curves into a simultaneous expression of systemic and pulmonary venous return (the venous return surface) resulted in a new framework of circulatory equilibrium, i.e., the extended Guyton's model [7]. Since the new framework has an analytical solution of circulatory equilibrium for a given set of ventricular and vascular mechanical properties, it provides us an extremely powerful tool in understanding the mechanisms how cardiac output is determined under a variety of pathological as well as physiological conditions.

III. FUTURE (2010~)

The extended Guyton's model enables us to qualitatively predict a circulatory equilibrium once the mechanical properties of the ventricular and vascular system are known. This helps understand how complex physiological regulatory systems such as baroreflex systems regulate the cardiovascular system. In a

preliminary study reported at this conference, we indicated that the extended Guyton's model is capable of quantitatively synthesizing dynamic baroreflex arterial pressure regulation on the basis of baroreflexly modulated ventricular and vascular mechanical properties.

The fact that we can quantitatively predict circulatory equilibrium for a given set of ventricular and vascular mechanical properties opens up vast clinical applications. If we can develop a feedback mechanism to manipulate mechanical properties of ventricle and vascular system, we can in turn feedback regulate the circulatory equilibrium, and thereby hemodynamics. Recently we developed a prototype of fully automated closed-loop treatment system that stabilizes hemodynamics of decompensated left heart failure. The system outperformed as good as well trained cardiologists [8].

The P-V relationship will remain to be a central theme that bridges basic cardiac physiology to extensive clinical applications.

IV. REFERENCES

[1] O. Frank, "Die Grundform des arteriellen Pulses," *Z Biol* 37: 483-526, 1899

[2] H. Suga, and K. Sagawa, "Instantaneous pressure-volume relationship and their ratio in the excised, supported canine left ventricle," *Circ Res 35: 117-127, 1974*

[3] H. Suga, T. Hayashi, M, Shirahata, and I. Ninomiya, "Critical evaluation of left ventricular systolic pressure-volume area as predictor of oxygen consumption rate," *Jpn J Physiol* 30: 907-919, 1980

[4] K. Sunagawa, W.L. Maughan, and K. Sagawa, "Left ventricular interaction with arterial load studied in isolated canine ventricle," *Am J Physiol 245 (Heart Circ Physiol 16):* H773-H780, 1983

[5] K. Sagawa, W.L. Maughan, H. Suga, and K. Sunagawa, "Cardiac contraction and end-systolic pressure-volume relationship," Oxford Press, 1988

[6] A.C. Guyton, "Determination of cardiac output by equating venous return curves with cardiac response curves," *Physiol Rev* 35: 123-129, 1955

[7] K. Uemura, M. Sugimachi, T. Kawada, A. Kamiya, Y. Jin, K. Kashihara, and K. Sunagawa, "A novel framework of circulatory equilibrium," *Am J Physiol Heart Circ Physiol* 286: H2376-H2385, 2004

[8] K. Uemura, A. Kamiya, I. Hidaka, T. Kawada, S. Shimizu, T. Shishido, M. Yoshizawa, M. Sugimachi and K. Sunagawa, "Automated drug delivery system to control systemic arterial pressure, cardiac output, and left heart filling pressure in acute decompensated heart failure," *J Appl Physiol 100:* 1278-1286, 2006

32nd Annual International Conference of the IEEE EMBS
Buenos Aires, Argentina, August 31 - September 4, 2010

Physiological Significance of Pressure-Volume Relationship: a Load-Independent Index and a Determinant of Pump Function

Masaru Sugimachi, *Member, IEEE*, Kenji Sunagawa, *Member, IEEE*,
Kazunori Uemura, and Toshiaki Shishido

***Abstract*—Pressure-volume relationship permits conceptual integration with time-varying elastance, stress-strain relationship, and pressure-volume area. It has also superior usefulness to other indexes, both as a load-independent index of ventricular contractility and as a determinant of ventricular pump function.**

PRESSURE-VOLUME relationship has become a standard framework [1] for discussing the mechanical properties of the ventricles and sometimes atria. It has gained popularity because of its conceptual integration and its superior usefulness, both as a load-independent index and as a determinant of pump function. The concept of pressure-volume relationship agrees with to that of time-varying elastance, that of (time-varying) material properties of myocardium (i.e., stress-strain relationship), and that of pressure-volume area as the major determinant of myocardial oxygen consumption [2].

A. A Load-Independent Index

Pressure-volume relationship (PVR), especially the end-systolic pressure-volume relationship (ESPVR), has been repeatedly shown as one of the least load-sensitive index of ventricular contractility. Although preload-recruitable stroke work (PRSW) has been a rival, it is obvious that PRSW would no longer be load insensitive in extreme cases such as isovolumic beats.

Although detailed examination of ESPVR revealed its load-dependence (such as deactivation and activation associated with ejection) and curvilinearity [3], ESPVR is still the least load-dependent index of ventricular contractility. The apparent linearity of ESPVR seems to be observed just by chance, taking into consideration that ESPVR can be reconstructed from nonlinear (exponential) end-systolic stress-strain relationship of myocardium.

The most important advance what the concept of PVR has provided are the decoupling of heart from vasculature (preload and afterload), and the fact that actively contracting tissue would change its mechanical properties in cardiac cycles. Decoupling the heart enabled us to separately discuss the changes in the heart and the vasculature, rather than mix them and discuss only the measured hemodynamic variables. The uncovered complex load-dependence and curvilinearity would have not sacrificed the value of decoupling. The concept of changeable material property has simplified the explanation of complex time course of pressure development and ejection.

B. A Determinant of Pump Function

ESPVR has provided a method to precisely predict the stroke volume for given end-diastolic volume, heart rate and afterload resistance. This was accomplished by recoupling ESPVR with effective arterial elastance (mainly determined by heart rate and resistance). This is a major advantage over PRSW. What is more, even the pressure and flow waveform can be reconstructed by recoupling time-varying PVR (for the entire cardiac cycle) and arterial high-resolution impedance [4].

Manuscript received April 7, 2009. This work was supported in part by Grant-in-Aid for Scientific Research (B 20300164) from the Ministry of Education, Culture, Sports, Science and Technology, by Health and Labour Sciences Research Grants (H20-katsudo-shitei-007) from the Ministry of Health Labour and Welfare of Japan.

M. Sugimachi, K. Uemura, and T. Shishido are with the National Cardiovascular Center Research Institute, Suita, Osaka 5658565, Japan (corresponding author Masaru Sugimachi to provide phone: +81-6-6833 -5012; fax: +81-6-6835-5403; e-mail: su91mach@ri.ncvc.go.jp).

K. Sunagawa is with Kyushu University, Fukuoka 8128582 Japan. (e-mail: sunagawa@cardiol.med.kyushu-u.ac.jp).

REFERENCES

[1] K. Sagawa, L. Maughan, H. Suga, and K. Sunagawa, "Cardiac Contraction and the Pressure-Volume Relationship," New York, Oxford University Press, 1988.

[2] H. Suga, "Ventricular energetics," *Physiol. Rev.* vol. 70, no. 2, 247–277, Apr. 1990.

[3] D. Burkhoff, S. Sugiura, D. T. Yue, and K. Sagawa, "Contractility-dependent curvilinearity of end-systolic pressure-volume relations," *Am. J. Physiol.* vol. 252, no. 6, part 2, H1218–H1227, Jun. 1987.

[4] T. W. Latson, W. C. Hunter, D. Burkhoff, K. Sagawa, "Time sequential prediction of ventricular-vascular interactions," *Am. J. Physiol.* vol. 251, no. 6, part 2, H1341–H1353, Dec. 1986.

32nd Annual International Conference of the IEEE EMBS
Buenos Aires, Argentina, August 31 - September 4, 2010

Automated drug delivery system for the management of hemodynamics and cardiac energetic in acute heart failure

Kazunori Uemura, Masaru Sugimachi, *Member, IEEE*,
Toru Kawada, and Kenji Sunagawa, *Member, IEEE*

Abstract— **We have developed a novel automated drug delivery system for simultaneous control of systemic arterial pressure (AP), cardiac output (CO), and left atrial pressure (P_{LA}) in acute heart failure. The circulatory equilibrium framework we established previously discloses that AP, CO, and P_{LA} are determined by equilibrium of the mechanical properties of the circulation, i.e. pumping ability of the left heart, stressed blood volume and systemic arterial resistance. Our system directly controls the three mechanical properties with cardiovascular drugs including inotropes and vasodilators, thereby controlling AP, CO, and P_{LA}. Furthermore, by precisely controlling bradycardia and LV inotropy, our system enables to improve cardiac energetic efficiency while preserving AP, CO, and P_{LA} within acceptable ranges. In conclusion, by directly controlling the mechanical properties of the heart and vessel, our automated system realizes comprehensive management of hemodynamics in acute heart failure.**

I. Introduction

In the management of patients with acute heart failure after myocardial infarction or following cardiac surgery, cardiovascular agents such as inotropes and/or vasodilators are commonly used to control systemic arterial pressure (AP), cardiac output (CO) and left atrial pressure (P_{LA}). Since responses to these agents vary between patients and within patient over time, strict monitoring of patient condition and frequent adjustments of drug infusion rates are usually required. This is a difficult and time-consuming process, especially in hemodynamically unstable patients.

Although several closed-loop systems [1, 2] to automate drug infusion have been developed to facilitate this process, no closed-loop system so far developed is capable of controlling the overall hemodynamics; i.e., controlling AP, CO and P_{LA} simultaneously. This is because all previous systems attempted to directly control AP and CO by estimating response of the variable to drug infusion [1, 2]. This approach is inapplicable because of the difficulties to estimate simultaneous AP, CO and P_{LA} responses to the infusion of multiple drugs.

In this study, we developed a new automated drug delivery system to control AP, CO and P_{LA} [3]. To overcome the difficulty of the previous systems, our system adopted a strikingly original approach. We previously developed a circulatory equilibrium framework by extending the Guyton's classic framework [4]. As shown in Fig. 1, the extended framework consists of an integrated cardiac output curve characterizing the pumping ability of the left and the right heart, and a venous return surface characterizing the venous return property of the systemic and pulmonary circulation [5-7]. The intersection point of the integrated CO curve and the venous return surface predicts the equilibrium point of CO, P_{LA} and right atrial pressure (P_{RA}) (Fig. 1). Once CO, P_{LA} and P_{RA} are predicted from the intersection point, systemic arterial resistance determines AP. Based on this framework, instead of directly controlling AP, CO, and P_{LA}, our system controls the integrated CO curve with dobutamine (DOB), the venous return surface with 10% dextran 40 (DEX) and furosemide (FUR), and systemic arterial resistance with sodium nitroprusside (SNP), thereby controlling AP, CO and P_{LA}. The purpose of this study was, therefore, to develop and validate the automated drug delivery system.

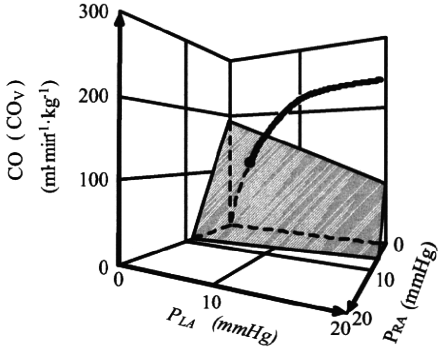

Fig. 1. Diagram of circulatory equilibrium for CO, venous return (CO_V), P_{LA}, and P_{RA}. The equilibrium CO, P_{LA} and P_{RA} are obtained as the intersection point of the venous return surface and integrated cardiac output curve.

Manuscript received April 23, 2010. This work was supported in part by Grant-in-Aid for Scientific Research (B 20300164, C 20500404) from the Ministry of Education, Culture, Sports, Science and Technology, by a research grant from Nakatani Foundation of Electronic Measuring Technology Advancement, by Health and Labour Sciences Research Grants (H20-katsudo-shitei-007) from the Ministry of Health Labour and Welfare of Japan.

K. Uemura, M. Sugimachi, and T. Kawada are with the National Cerebral and Cardiovascular Center Research Institute, Suita, Osaka 5658565, Japan.

K. Sunagawa is with Kyushu University, Fukuoka 8128582 Japan.

(corresponding author Kazunori Uemura, MD, PhD to provide phone: +81-6-6833-5012; fax: +81-6-6835-5403; e-mail: kuemura@ri.ncvc.go.jp).

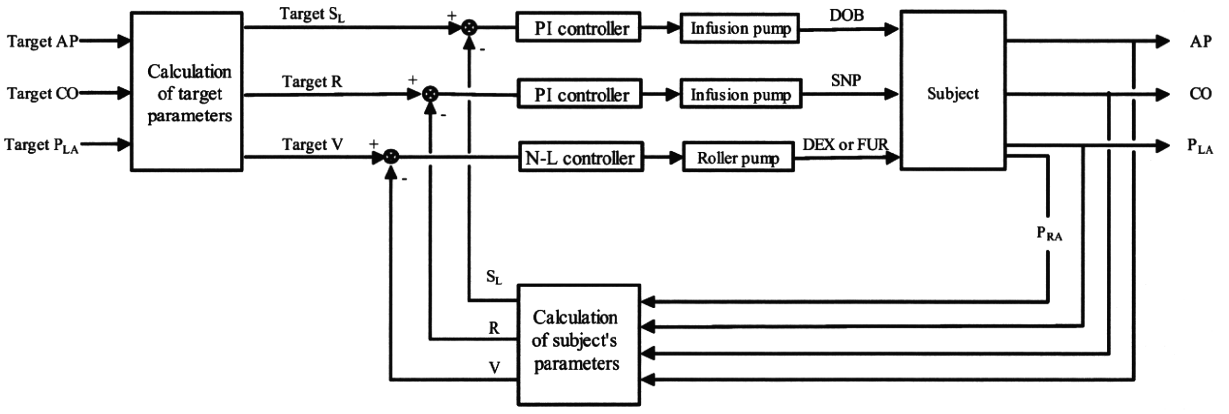

Fig. 2. Schematic illustration of an automated drug delivery system for simultaneous control of AP, CO and P_{LA}. Proportional-integral (PI) feedback controllers adjust infusion rate of DOB and SNP to minimize the difference between target and subject's S_L and those of R, respectively. Nonlinear (N-L) feedback controller adjusts infusion of DEX or injection of FUR to minimize the difference between target and subject's V.

In acute heart failure, cardiac energetic efficiency should also be improved. Theoretically, if heart rate (HR) is reduced while AP, CO and P_{LA} are maintained by preserving S_L with precisely increased LV contractility, it is possible to improve cardiac energetic efficiency and reduce LV oxygen consumption per minute (MVO_2) [8]. In the present study, we also investigated whether this hemodynamics can be accomplished in acute heart failure using our automated drug delivery system.

II. Methods

A. Automated drug delivery system

The integrated CO curve is parameterized by the pumping ability of the left heart (S_L) [ml·min^{-1}·kg^{-1}], the venous return surface by total stressed blood volume (V) [ml·kg^{-1}], and the systemic arterial resistance by R [mmHg·ml^{-1}·min·kg], which are calculated for a given set of AP, CO, P_{LA} and P_{RA} as the following formulas [3];

$$S_L = CO/[\ln(P_{LA} - 2.03) + 0.8] \quad (1)$$

$$V = (CO + 19.61P_{RA} + 3.49P_{LA}) \times 0.129 \quad (2)$$

$$R = (AP - P_{RA})/CO \quad (3)$$

Fig. 2 is a schematic illustration of the automated drug delivery system [3]. Once target values for AP, CO and P_{LA} are defined and fed into the computer, it calculates the target values for S_L, R, and V using Equations (1)-(3). The subject's S_L, R, and V are calculated from measured AP, CO and P_{LA} values using Equations (1)-(3). To minimize the differences between target and subject's S_L and R, proportional-integral feedback controllers adjust the infusion rates of DOB and SNP, respectively. To minimize the difference between target and subject's V, a nonlinear feedback controller adjusts the infusion of DEX or injection of FUR. Gain and rules of the controllers were predefined on the basis of the step responses of S_L, R, and V to the infusions of the drugs [3].

The adjustment processes are repeated in parallel and continued until the differences disappear.

B. Animal experiments to validate performance of the automated drug delivery system

In 12 anesthetized dogs, we acutely created ischemic heart failure by coronary embolization, which decreased CO from 133 ± 42 to 69 ± 22 ml·min^{-1}·kg^{-1}, AP from 109 ± 18 to 91 ± 17 mmHg and increased P_{LA} from 7 ± 2 to 19 ± 6 mmHg.

We connected the animals to the system, and defined target AP (90-105 mmHg), target CO (90-100 ml·min^{-1}·kg^{-1}) and target P_{LA} (8-12 mmHg), which were fed into the system to determine target values for S_L, R, and V as described above. The controllers were then activated by closing the loops. We observed the performance of the system over 50-60 min.

C. Circulatory equilibrium and cardiac energetics

S_L is theoretically related with LV end-systolic elastance (E_{es}, an index of LV contractility), HR, R and diastolic myocardial stiffness (k) as the following formula [7]

$$S_L = \frac{1}{k} \cdot \frac{E_{es}}{(E_{es}/HR) + R} \quad (4)$$

LV Stroke work (SW) is expressed as

$$SW = (AP - P_{LA}) \cdot CO/HR \quad (5)$$

LV pressure-volume area (PVA, an index of total mechanical energy of LV contraction) can be expressed as

$$PVA = AP \cdot AP/2E_{es} + SW \quad (6)$$

LV oxygen consumption per beat (BVO_2) is related to PVA and E_{es} as follows

$$BVO_2 = \alpha \cdot PVA + \beta \cdot E_{es} + \gamma \quad (7)$$

where α, β, and γ are constants. LV mechanical efficiency (ME) and oxygen consumption per minute (MVO_2) are expressed as follows:

$$ME = SW/BVO_2 \quad (8)$$

$$MVO_2 = BVO_2 \cdot HR \quad (9)$$

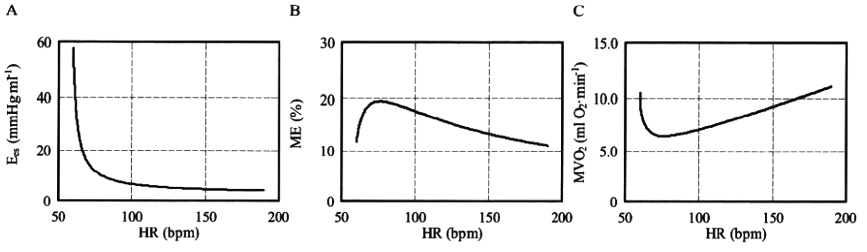

Fig. 3. Simulated relations of heart rate (HR) with left ventricular end-systolic elastance (E_{es}) (**A**), left ventricular mechanical efficiency (ME) (**B**), and left ventricular oxygen consumption per minute (MVO_2) (**C**), when AP, CO and P_{LA} are kept at fixed values.

Using Equations (4)-(9) and fixed values of AP (100 mmHg), CO (100 ml·min^{-1}·kg^{-1}) and P_{LA} (10 mmHg), we numerically simulated the individual relations of HR with E_{es}, ME and MVO_2 (Fig. 3). In these computations, representative k, α, β and γ values (not shown) were used, which are appropriate for a 20-kg dog.

As indicated in Fig. 3, HR is inversely related to E_{es} (Fig. 3A). Over the physiological range of HR for dogs (>80 bpm), ME increases as HR is reduced (Fig. 3B), i.e. cardiac energetic efficiency is optimized. At HR of 75 bpm, ME becomes maximal and MVO_2 becomes minimal (Fig. 3B, C). When HR is reduced from 150 to 110 bpm, E_{es} increases from 4.6 to 5.9 mmHg·ml^{-1} (29% increase) and ME increases from 13 % to 17 % (24 % increase), whereas MVO_2 decreases from 8.9 to 7.2 ml O_2·min^{-1} (19% reduction) [8]. This indicates that as long as HR is within the physiological range, HR reduction together with compensatory LV inotropy (an increase of E_{es}) consistently improves cardiac energetic efficiency and reduces MVO_2.

D. Animal experiments to optimize cardiac energetics using the automated drug delivery system

In 7 anesthetized dogs, we acutely created ischemic heart failure by coronary embolization, which decreased CO from 101±5 to 62±13 ml·min^{-1}·kg^{-1}, AP from 114±4 to 97±14 mmHg and increased P_{LA} from 9 ± 1 to 17±2 mmHg. Zatebradine (0.5 mg·kg^{-1}) was administered intravenously to suppress the intrinsic atrial beat, and atrial pacing was then initiated to control HR (146±8 bpm). After induction of acute heart failure, cardiac energetics were evaluated (*AHF*).

We activated the system with target values of 90-100 mmHg for AP, 80-100 ml/kg/min for CO and 10-12 mmHg for P_{LA}. The system restored AP, CO and P_{LA} to their respective target values within 30 min. After confirming stable hemodynamics, cardiac energetics were evaluated (*Initial HR*). We then reduced the pacing rate in steps of 10 or 20 bpm. The maximum HR reduction (*Lowest HR*) averaged 39±12 bpm. For each HR step, we waited for hemodynamic stabilization, and the measurements of cardiac energetics were performed.

III. Results

A. Performance of the automated drug delivery system

Fig. 4 shows the experimental trial in a representative animal. The system was activated at 0 min. Fig. 4A shows the time courses of the infusion rates of DOB and SNP, and the accumulated volume of infused DEX. In this case, FUR was not injected. Fig. 4B shows the time courses of S_L, R and V. Infusion rates of DOB, SNP, and DEX were adjusted so that S_L, R and V reached their respective target values. By controlling the cardiovascular parameters, the automated system controlled AP, CO and P_{LA} accurately and stably as demonstrated in Fig. 4C. AP, CO and P_{LA} reached their respective target levels within 30 min and remained at these levels.

In 12 animals, the average times for AP, CO and P_{LA} to reach the acceptable ranges (± 10 mmHg of target AP, ± 10 ml·min^{-1}·kg^{-1} of target CO, ± 2 mmHg of target P_{LA}) were 5.2 ± 6.6 min, 6.8 ± 4.6min, and 11.7 ± 9.8 min, respectively. The average standard deviations from the target values were small for AP [4.4 ± 2.6mmHg], CO [5.4 ± 2.4ml·min^{-1}·kg^{-1}] and P_{LA} [0.8 ± 0.6 mmHg].

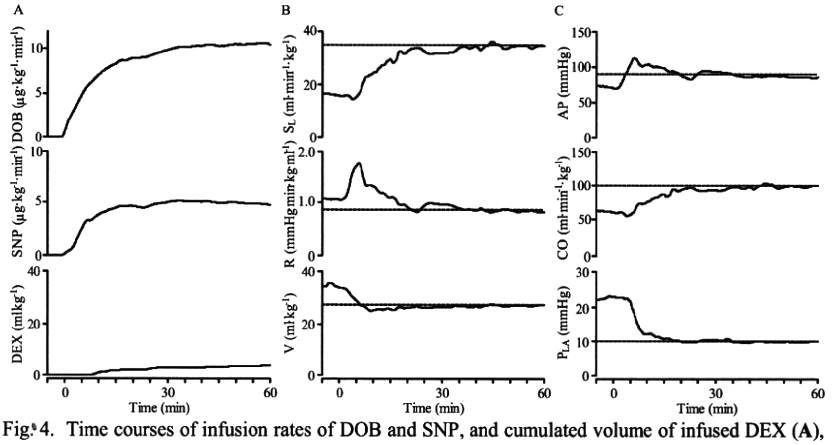

Fig. 4. Time courses of infusion rates of DOB and SNP, and cumulated volume of infused DEX (**A**), cardiovascular parameters (**B**), and hemodynamic variables (**C**) in one representative animal during closed-loop control of hemodynamics. Broken horizontal lines in panel B and C indicate target values.

B. Cardiac energetics improved following bradycardia while preserving normal hemodynamics in heart failure

In seven anesthetized dogs with acute heart failure, the automated drug delivery system restored and maintained normal hemodynamics (CO; 88±3 ml·min^{-1}·kg^{-1}, P_{LA};

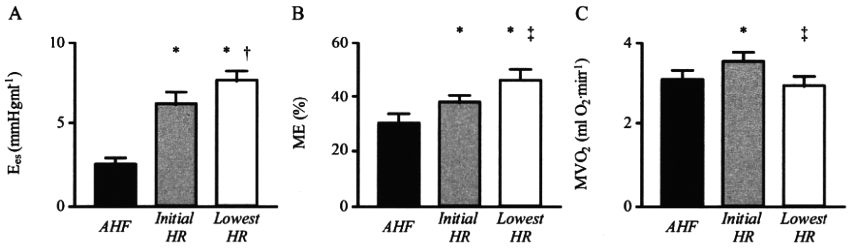

Fig. 5. Cardiac energetics after coronary artery embolization (*AHF*), at the initial HR (*Initial HR*), and at the lowest HR (*Lowest HR*). E_{es}, left ventricular (LV) end-systolic elastance; ME, LV mechanical efficiency; MVO_2, LV oxygen consumption per minute. Data are means ± SEM. *: $P<0.01$ vs *AHF*. †: $P<0.05$, ‡: $P<0.01$ versus *Initial HR*.

10.9±0.4 mmHg), even when zatebradine significantly reduced HR (107±7 bpm, -27±3%).

Fig. 5 summarizes cardiac energetics at *AHF*, *Initial HR*, and *Lowest HR*. When the data at *Initial HR* and *Lowest HR* were compared with those at *AHF*, E_{es} and ME increased significantly. MVO_2 at *Initial HR* also increased compared to that at *AHF*, although MVO_2 at *Lowest HR* was almost identical to that at *AHF*. The automated drug delivery system restored normal hemodynamics with increased energy cost at *Initial HR*, but with diminished energy cost at *Lowest HR*. Comparing the data at *Lowest HR* with those at *Initial HR*, E_{es} increased (+34±14 %), ME increased (+22±6 %) and MVO_2 decreased significantly (-17±4 %). Changes in the LV mechanoenergetic data following HR reduction averaged over seven animals are compatible with those predicted theoretically (Fig. 3).

IV. Discussion

A. Characteristics of our system

Our system controls the mechanical determinants of circulation, and as a result achieves target values for hemodynamic variables [3]. Previous systems attempted to control hemodynamic variables by estimating the apparent input–output relations between drug infusion and response of the controlled variables. In the systems that control AP and CO, all possible input–output relations have to be estimated; namely, inotrope–AP, inotrope–CO, vasodilator–AP, and vasodilator–CO relations [2]. The reason is that these drugs affect AP and CO simultaneously to almost the same degree. If this previous approach is applied to simultaneous control of AP, CO and P_{LA}, at least 9 input–output relations have to be estimated, since at least 3 drugs are required to independently control the three variables. This would make the system extremely complicated, and therefore be practically unfeasible. The three drug controllers in our system (Fig. 2) are designed on the basis of only three input–output relations between drug infusion and response of the controlled parameter; namely, DOB–S_L, SNP–R and DEX/FUR–V. The fact that the three closed loops are effectively decoupled simplifies the entire system. This also permits a system operator, who would be a physician untrained in control engineering, to understand its behavior easily

B. Simultaneous optimization of cardiac energetic and hemodynamics

The degree of reduction in MVO_2 (17 %, *Lowest HR* vs *Initial HR* in Fig. 5C) when HR was reduced by 30% in the present experiment is less than that observed in beta-blockade treatment. For example, atenolol decreased MVO_2 by 40% when HR was reduced by 30% in dogs during exercise. Negative ventricular inotropy accompanying HR reduction accounts for the further reduction in MVO_2 achieved by beta-blockade. However, in acute heart failure, use of beta-blockers is contraindicated owing to its adverse effects on systemic hemodynamics. Taken together, the degree of reduction in MVO_2 obtained in this study is reasonable considering that it is achieved without sacrificing the normal hemodynamic condition.

V. Conclusion

By directly controlling the mechanical properties of the heart and vessel, our automated system enables comprehensive management of hemodynamics in acute heart failure.

References

[1] W. R. Chitwood Jr., D. M. Cosgrove 3rd., R. M. Lust, "Multicenter trial of automated nitroprusside infusion for postoperative hypertension. Titrator Multicenter Study Group," *Ann. Thorac. Surg.* vol. 54, no. 3, 517-522, Sep. 1992.

[2] C. Yu, R. J. Roy, H. Kaufman, B. W. Bequette, "Multiple-model a daptive predictive control of mean arterial pressure and cardiac output," *IEEE. Trans. Biomed. Eng.* vol. 39:765-778, 1992.

[3] K. Uemura, A. Kamiya, I. Hidaka, T. Kawada, S. Shimizu, *et al.*, "Automated drug delivery system to control systemic arterial pressure, cardiac output, and left heart filling pressure in acute decompensated heart failure," *J. Appl. Physiol.* vol. 100, no 4, 1278-1286, Apr. 2006.

[4] A. C. Guyton, "Determination of cardiac output by equating venous return curves with cardiac response curves," *Physiol. Rev.* vol. 35, no. 1,123–129, Jan. 1955.

[5] K. Sunagawa, K. Sagawa, W. L. Maughan, "Ventricular interaction with the loading system," *Ann. Biomed. Eng.* vol. 12, no. 2, 163-189, 1984.

[6] K. Uemura, M. Sugimachi, T. Kawada, A. Kamiya, Y. Jin, *et al.*, "A novel framework of circulatory equilibrium," *Am. J. Physiol. Heart Circ. Physiol.* vol. 286, no. 6, pp. H2376–H2385, Jun. 2004.

[7] K. Uemura, T. Kawada, A. Kamiya, T. Aiba, I. Hidaka, *et al.*, "Prediction of circulatory equilibrium in response to changes in stressed blood volume," *Am. J. Physiol. Heart Circ. Physiol.* vol. 289, no. 1, H301–H307, Jul. 2005.

[8] K. Uemura, K. Sunagawa, M. Sugimachi, "Computationally managed bradycardia improved cardiac energetics while restoring normal hemodynamics in heart failure," *Ann. Biomed. Eng.* vol. 37, no. 1, 82-93, Jan. 2009.

32nd Annual International Conference of the IEEE EMBS
Buenos Aires, Argentina, August 31 - September 4, 2010

Estimated Venous Return Surface and Cardiac Output Curve Precisely Predicts New Hemodynamics after Volume Change

Masaru Sugimachi, *Member, IEEE*, Kenji Sunagawa, *Member, IEEE*,
Kazunori Uemura, Atsunori Kamiya, Shuji Shimizu, Masashi Inagaki and Toshiaki Shishido

***Abstract*— In our extended Guyton's model, the ability of heart to pump blood is characterized by a cardiac output curve and the ability of vasculature to pool blood by a venous return surface. These intersect in a three-dimensional coordinate system at the operating right atrial pressure, left atrial pressure, and cardiac output. The baseline cardiac output curve and venous return surface and their changes after volume change would predict new hemodynamics. The invasive methods needed to precisely characterize cardiac output curve and venous return surface led us to aim at estimating cardiac output curve and venous return surface from a single hemodynamic measurement. Using the average values for two logarithmic function parameters, and for two slopes of a surface, we were able to estimate cardiac output curve and venous return surface. The estimated curve and surface predicted new hemodynamics after volume change precisely.**

I. Introduction

OUR group has developed an extended Guyton's cardiovascular model, where the ability of the right- and left-sided heart to pump blood is integratively characterized by a single curve (cardiac output curve) and the ability of vasculature to pool blood is expressed as a surface (venous return surface). The cardiac output curve and the venous return surface intersect in a three-dimensional coordinate system, and the three coordinates show the operating right atrial pressure (RAP), left atrial pressure (LAP), and cardiac output (CO), respectively (Fig. 1).

If one knows the baseline cardiac output curve and venous return surface and how these change after volume infusion and depletion, one can predict new hemodynamics by combining a new cardiac output curve and a new venous return surface. The precise characterization of cardiac output curve and venous return surface, however, needs extremely invasive measures for changing loading conditions to be applicable to patients with heart diseases (see Sections IIB and IIC for the detailed invasive methods used in animal experiments). Therefore, the aim of this study was to circumvent this difficulty by establishing a method to approximately obtain the cardiac output curve and venous return surface from a single hemodynamic measurement.

Manuscript received April 7, 2009. This work was supported in part by Grant-in-Aid for Scientific Research (B 20300164, C 20500404) from the Ministry of Education, Culture, Sports, Science and Technology, by Health and Labour Sciences Research Grants (H20-katsudo-shitei-007) from the Ministry of Health Labour and Welfare of Japan.

M. Sugimachi, K. Uemura, A. Kamiya, S. Shimizu, M. Inagaki and T. Shishido are with the National Cardiovascular Center Research Institute, Suita, Osaka 5658565, Japan (corresponding author Masaru Sugimachi to provide phone: +81-6-6833-5012; fax: +81-6-6835-5403; e-mail: su91mach@ri.ncvc.go.jp).

K. Sunagawa is with Kyushu University, Fukuoka 8128582 Japan. (e-mail: sunagawa@cardiol.med.kyushu-u.ac.jp).

II. Model and Methods

A. Extended Guyton's Model

We have extended Guyton's model [1] to handle a number of difficulties frequently encountered in clinical settings in patients with predominantly unilateral heart failure.

First, we extended a 2D (RAP-CO) Guyton's model to a 3D (RAP-LAP-CO) model, and introduced a third axis for LAP (Fig. 1) [2], [3]. By this modification, we can get the operating LAP directly from the intersection between cardiac output curve and venous return surface. LAP indicates the degree of pulmonary congestion and inadequate blood oxygenation, and normal range of LAP is as important as that of cardiac output and that of blood pressure for sustaining life.

Second, in this 3D model, we can separately express the changes in pumping ability of the right- and left-sided heart; the 3D cardiac output curve (Fig. 1, thick curve) is, in reality, the integration of two separate 2D cardiac output curves. The pumping ability of the right-sided heart can be obtained by projecting the 3D curve to the RAP-CO plane, and that of the

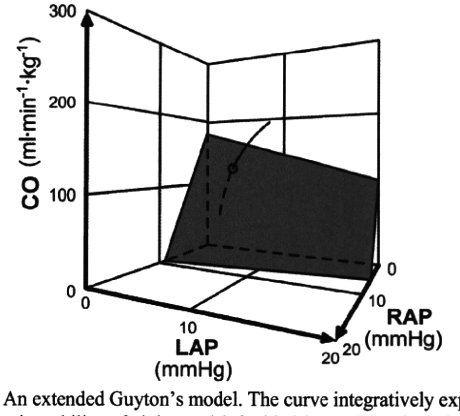

Fig. 1. An extended Guyton's model. The curve integratively expresses the pumping ability of right- and left-sided heart. The shaded surface characterizes the blood-pooling ability of the vasculature. RAP, right atrial pressure; LAP, left atrial pressure; CO, cardiac output (per kg of body weight).

left-sided heart can be obtained by projecting it to the LAP-CO plane. The preferential decrease in the pumping ability of the left-sided heart, such as seen in the ischemic heart disease, would rotate the projected curve to the RAP-LAP plane to the direction of LAP axis.

Third, the blood-pooling ability of the vasculature and the effect of stressed blood on the vasculature can be expressed by the venous return surface (Fig. 1, shaded surface). This surface remains the same so long as the total stressed volume is unchanged irrespective of its distribution. Increased LAP and pulmonary congestion associated with left-sided heart failure is characterized by blood redistribution from systemic to pulmonary vascular beds. Blood redistribution, however, would not change the venous return surface itself (i.e., unaffected by the changes in pumping ability). This is in sharp contrast with the classical venous return curve of Guyton's model. The relatively flat slope of the surface to the direction of LAP axis indicates the smaller blood-pooling ability of pulmonary vascular beds. As a result, the decrease in RAP with systemic-to-pulmonary blood redistribution is much smaller than the increase in LAP. This is shown, also illustratively in Fig. 1, by moving along the venous return surface and parallel to the RAP-LAP plane (keeping CO constant).

B. Animal Experiments to Characterize Cardiac Output Curve

We planned to characterize both cardiac output curve and venous return surface as precisely as possible in animals by using even the most invasive methods. In characterizing the pumping ability, only the heart of animals is needed; in characterizing the blood-pooling ability, only the vasculature of animals is needed.

The experiment for the characterization of cardiac output curve was less invasive. We do not need to physically detach the vasculature from the heart. Rather, in 7 dogs, by withdrawing and transfusing blood in a stepwise manner, we were able to obtain both right- and left-sided cardiac output curve simultaneously.

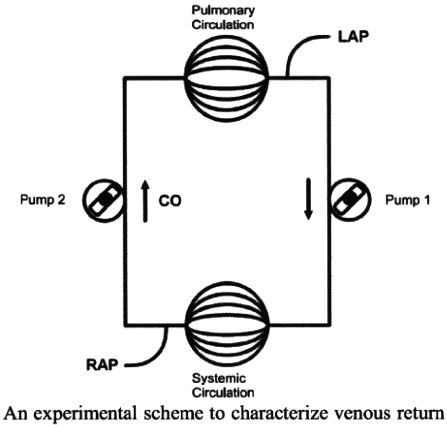

Fig. 2. An experimental scheme to characterize venous return surface. By replacing the right- and the left-sided heart with respective roller pumps, one can change cardiac output of the right- and the left-sided heart independently.

C. Animal Experiments to Characterize Venous Return Surface

Figure 2 depicts the scheme of an experiment to characterize the venous return surface. To extract only the vasculature and to physically remove the animal heart from the cardiovascular system, we replaced the right- and the left-sided heart with respective roller pumps. These pumps allow us to change CO of the right- and left-sided heart independently. Changing the flow of the two pumps at the same level would simulate the weak or strong heart. Transient unbalancing flow would redistribute blood between systemic and pulmonary vascular beds.

In each of 6 canine preparations, we obtained 6 different hemodynamic (CO, RAP, LAP) data sets. In each animal, these sets of data were fit to a flat surface in 3D coordinate system by linear regression analysis. CO was selected as a dependent variable and RAP (~2-5 mmHg) and LAP (~0-10 mmHg) are selected as independent variables.

D. Method to Estimate Cardiac Output Curve from a Single Hemodynamic Data Set

We fit experimental data to two logarithmic curves (one for the right- and the other for the left-sided heart), based on the knowledge of exponential end-diastolic pressure volume relationship and linear end-systolic pressure volume relationship, as follows.

$$CO = S\,[\ln(P - A) + B]$$

Here, P indicates RAP or LAP; A, B, and S are parameters. As analytical solution indicated that A and B is only dependent on diastolic properties of the ventricles, and is unlikely to change acutely, we fixed these parameters as their respective average values. This enabled one to estimate cardiac output curve from a single hemodynamic data set.

E. Method to Estimate Venous Return Surface from a Single Hemodynamic Data Set

We were able to fit experimental data to a flat surface well (r^2=0.92 to 0.99). As the surfaces from 6 animals were reasonably parallel (see Results), we used average slopes to estimate venous return surface from a single hemodynamic data set. Furthermore, as CO-axis intercept was linearly related to the withdrawn or transfused blood volume, we used this relationship to estimate a new venous return surface after blood volume change.

III. RESULTS

A. Method to Estimate Cardiac Output Curve from a Single Hemodynamic Data Set

We were able to fit the cardiac output curve of both the right- and the left-sided heart by logarithmic functions (right-sided heart, r^2=0.90 to 0.99; left-sided heart, r^2=0.95 to 0.99). Since standard deviation of parameter A (1.29) or that of parameter

B (1.25) was much smaller than that of parameter S (30.9), we used the respective average values for A and B. The obtained cardiac output curves for right- and left-sided heart were as follows.

$$CO = S_R [\ln(RAP - 2.13) + 1.90] \quad (1)$$

$$CO = S_L [\ln(LAP - 2.03) + 0.80] \quad (2)$$

Parameters S_R and S_L can be used to represent the magnitude of the pumping ability of the right- and left-sided heart, respectively. As S_R and S_L can be calculated from a single set of hemodynamic data, we can approximately get cardiac output curve.

B. Method to Estimate Cardiac Output Curve from a Single Hemodynamic Data Set

In Figure 3 we have shown the venous return surfaces obtained from all 6 dogs. The surfaces were shown (as if they were lines) from the direction parallel to the surface. The figure indicates that in each of 6 dogs, all 6 data sets are located very near the flat surface. This implied the goodness of the fit of these data points to the flat surface. It is also shown that three coordinate axes are almost parallel among these dogs. This is because the slopes of the surface were almost the same among animals. These experimental results indicated that the venous return surface is linear and can be expressed by a common equation for all animals.

$$CO = CO_{max} - 19.61\ RAP - 3.49\ LAP.$$

Further, by infusing or withdrawing known amounts of blood, we were able to relate CO_{max} to blood volume as

$$CO_{max} = V / 0.129 \quad (3)$$

where V is total intravascular stressed blood volume. Combining these equations resulted in

$$CO = V / 0.129 - 19.61\ RAP - 3.49\ LAP. \quad (4)$$

Parameter V can be used to monitor the changes in total stressed blood volume. As V can be calculated from a single set of hemodynamic data, we can approximately get venous return surface.

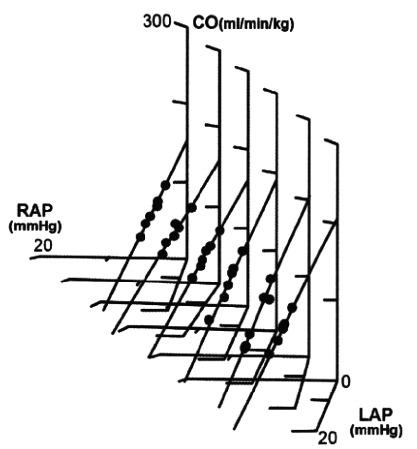

Fig. 3. Venous return surfaces obtained from 6 dogs. For each dog, the venous return surface was projected in a direction parallel to the surface, and was superimposed with each other.

C. Prediction of New Hemodynamics after Volume Change

We predicted new hemodynamics after volume change as follows. First, baseline cardiac output curve (Equations 1 and 2) and venous return surface (Equation 4) were approximately estimated from a single baseline hemodynamic data, by the methods shown in two previous sections IIIA and IIIB. Next, a new venous return surface was estimated by changing CO_{max} according to Equation 3. We assumed that cardiac output curve would not change by the volume change. Finally, new hemodynamics data were estimated by calculating the intersection between cardiac output curve and venous return surface.

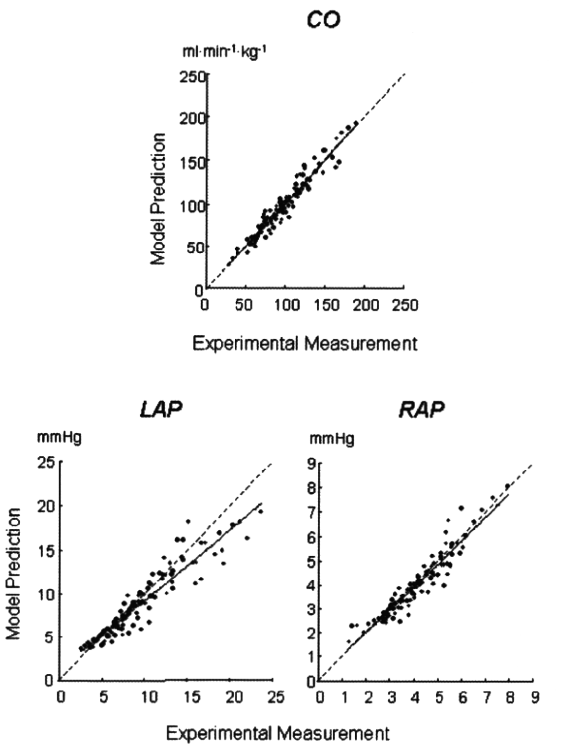

Fig. 4. Prediction of CO, LAP, and RAP from estimated cardiac output curve and venous return surface after volume change.

Using these new estimated cardiac output curve and venous return surface, we were able to predict the hemodynamics (y value) after withdrawal or transfusion of blood of known volume precisely as compared to actually measured (x value) (CO: $y = 0.93x + 6.5$, $r^2 = 0.96$, SEE [standard error of estimate] = 7.5 $ml \cdot min^{-1} \cdot kg^{-1}$; LAP: $y = 0.90x + 0.5$, $r^2 = 0.93$, SEE = 1.4 mmHg; RAP: $y = 0.87x + 0.4$, $r^2 = 0.91$, SEE = 0.4 mmHg) (Fig. 4) [3].

IV. Discussion

A. Most Undiagnosed Property: Total Stressed Blood Volume

The three major players of the cardiovascular system are heart

(pumps), vasculature (tubes with resistive and capacitive function), and blood. These three components interactively determine all hemodynamic variables. Of these, pump function and resistive function of vasculature have been repeatedly evaluated in previous studies. These properties were also evaluated clinically.

In contrast, evaluation of the vascular capacitive function and that of the blood volume have been relatively ignored. Even though blood volume drastically changes, there have been no reasonable methods to evaluate total stressed blood volume precisely. Simple measurement of central venous pressure (i.e., RAP) cannot be a proxy marker of blood volume, as this pressure value also changes with pump function or with redistribution of blood.

It is clear from our results [$V = (CO + 19.61\ RAP + 3.49\ LAP) \times 0.129$] that blood volume (V) is not solely determined by RAP. Rather, all three variables CO, RAP and LAP contribute (not as differently as have been considered) to the changes in blood volume. Clinicians should know that when LAP increases by 5.6 mmHg, or CO increases by 0.98L/min in 50-Kg patients, similar blood volume increases as RAP is increased by 1 mmHg.

Implantable devices with volume monitoring functionality for patients with heart failure should also take these results into consideration.

B. Hemodynamic Variables and Cardiovascular Properties

In clinical practice, physicians have to restore hemodynamic variables to their respective normal range. Of these, the most important three variables include blood pressure, CO and LAP. These variables are essentially important as blood pressure determines the perfusion of vital organs (for short-term need), CO determines the perfusion of peripheral tissues (for long-term need), and LAP determines blood oxygenation in lungs.

These hemodynamic variables are, in turn, determined by the interaction between cardiovascular properties, such as pump, resistance, capacitance, and blood volume. What clinicians should know, monitor, and correct are in reality these cardiovascular properties. Most drugs and interventions are aimed at correcting mainly one of these properties. From these viewpoints, the method to continuously estimate cardiovascular properties from measured hemodynamics is the most basic need in patient monitoring.

V. Conclusion

We have successfully developed a method to estimate the cardiac output curve and venous return surface from a single hemodynamic data set. This method enabled to predict new hemodynamics after withdrawal or transfusion of blood of known volume.

References

[1] A. C. Guyton, "Determination of cardiac output by equating venous return curves with cardiac response curves," *Physiol. Rev.* vol. 35, no. 1,123–129, Jan. 1955.

[2] K. Uemura, M. Sugimachi, T. Kawada, A. Kamiya, Y. Jin, *et al.*, "A novel framework of circulatory equilibrium," *Am. J. Physiol. Heart Circ. Physiol.* vol. 286, no. 6, pp. H2376–H2385, Jun. 2004.

[3] K. Uemura, T. Kawada, A. Kamiya, T. Aiba, I. Hidaka, *et al.*, "Prediction of circulatory equilibrium in response to changes in stressed blood volume," *Am. J. Physiol. Heart Circ. Physiol.* vol. 289, no. 1, H301–H307, Jul. 2005.

32nd Annual International Conference of the IEEE EMBS
Buenos Aires, Argentina, August 31 - September 4, 2010

How to quantitatively synthesize dynamic changes in arterial pressure from baroreflexly modulated ventricular and arterial properties

Takafumi Sakamoto, Yoshinori Murayama, Tomoyuki Tobushi, Kazuo Sakamoto, Atsushi Tanaka, Takaki Tsutsumi, and Kenji Sunagawa, Senior *Member, IEEE*

***Abstract*—Baroreflex regulates arterial pressure by modulating ventricular and vascular properties. We investigated if the framework of circulatory equilibrium that we developed previously (Am J Physiol 2004, 2005) by extending the classic Guyton's framework is capable of predicting baroreflex induced changes in arterial pressure. In animal experiments, we estimated open loop transfer functions of baroreflexly modulated ventricular and vascular properties, synthesized baroreflex induced dynamic changes in arterial pressure using the estimated transfer functions and compared the predicted responses with measured responses. We demonstrated that the predicted baroreflex induced changes in arterial pressure matched reasonable well with those measured. We conclude that the framework of circulatory equilibrium is generalizable under the condition where baroreflex dynamically changes arterial pressure.**

I. Introduction

Baroreflex is known to be the fastest mechanism in the body to stabilize arterial pressure (AP). This AP stabilization is achieved by feedback regulation of ventricular and vascular properties [1-3]. However, how those changes in mechanical properties quantitatively impact AP remains unknown. We previously developed a framework of circulatory equilibrium where we introduced the left atrial pressure-cardiac output (CO) relationship into the classic Guyton's framework and expanded the venous return (VR) curve to the VR surface. We then expressed the CO curves and VR surface using end-systolic elastance (Ees), heart rate (HR), vascular resistance (R) and stressed blood volume (V) [4, 5] and derived the circulatory equilibrium as the intersection between the CO curve and VR surface. The purpose of this investigation is if the extended Guyton's framework can quantitatively predict dynamic AP responses by incorporating the baroreflexly modulated ventricular and arterial properties.

Manuscript received April 23, 2010. This work was supported in part by Health and Labour Sciences Research Grant for Research on Medical Devices for Improving Impaired QOL from the Ministry of Health Labour and Welfare of Japan, Health and Lobour Sciences Research Grant for Clinical Research from the Ministry of Health Labour and Welfare of Japan, and Grant-in-Aid for Scientific Research(S) (18100006) from the Japan Society for the Promotion of Science

T. Sakamoto, Y. Murayama, T. Tobushi, K. Sakamoto, A. Tanaka and K. Sunagawa are with Kyushu university, Fukuoka 8128582 Japan. (corresponding author Takafumi Sakamoto to provide phone: +81-92-642-5360; fax: +81-92-642-5357; e-mail: tsaka@cardiol.med.kyushu-u.ac.jp).

T. Tsutsumi is with Iizuka Hospital, Iizuka 8208505 Japan (e-mail: tsutsumi@cardiol.med.kyushu-u.ac.jp).

II. Methods

A. A framework of circulatory equilibrium

The framework of circulatory equilibrium consists of the VR surface representing VR of the systemic and pulmonary circulations and the integrated CO curve representing the pumping ability of the left (LV) and right ventricle (RV) (Fig. 1) [4, 5]. The integrated CO curve and VR surface (CO*v*) are formulated as

$$CO = \frac{1}{k} \times \frac{Ees}{Ees/HR + R} \times \{\log(Pat - F) + H\}$$

and

$$COv = V/w - Gp \times P_{LA} - Gs \times P_{RA}$$

respectively, where Pat is left atrial pressure (P_{LA}) for LV and right atrial pressure (P_{RA}) for RV. k, F, H, w, Gp and Gs are empirically derived constants. Once we obtain a set of Ees, R, HR and V, we derive CO by the framework and estimate AP by multiplying CO and R [4, 5].

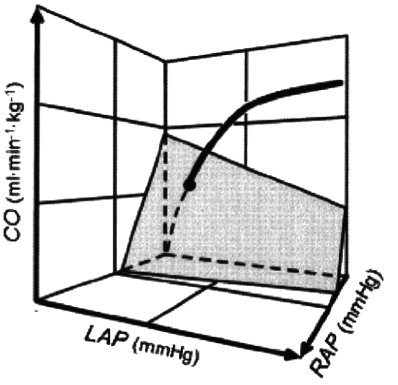

FIG.1 A FRAMEWORK OF CIRCULATORY EQUILIBRIUM

B. Animal preparation

Animal care was in accordance with institutional guidelines. Six mongrel dogs weighing 16.5±1.2kg (mean±SD) were anesthetized with pentobarbital sodium. We cut the vagosympathetic trunk to eliminate other reflexes and isolated

the bilateral carotid sinuses from the systemic circulation and connected them to a servo pump to control intrasinus pressure (CSP). An ultrasonic flow probe was placed around the ascending aorta to measure CO. We implanted two pairs of sonomicrometer in the epicardium and inserted a micromanometer into LV via the apex to measure Ees. We measured AP, P_{LA} and P_{RA}. Stressed blood volume was estimated from the VR surface. All analog data were digitalized at 200Hz with 12-bit resolution.

C. *Identification of the transfer function*

We perturbed CSP with pseudorandom binary sequences (100 and 180 mmHg) with a shortest interval of 5 seconds to identify the open-loop transfer functions from CSP to Ees, HR, R and V. We estimated the transfer functions in the frequency range between 0.002 to 0.1 Hz. To quantify the linear dependence between the input and output signals in the frequency domain, we also estimated a magnitude-squared coherence function.

D. *Prediction of the dynamic change of AP*

To validate the framework of circulatory equilibrium, we predicted Ees, HR, R and V using those estimated transfer functions in response to changes in CSP in data sets that had not been used to estimate the transfer functions. We then predicted APs using the developed framework and compared them against measured.

III. Results

Mean AP, HR, Ees, R and V during perturbations were 124±22 mmHg, 168±13 bpm, 11.3±2.9 mmHg/ml, 1.37±0.27 ml/(ml/min/kg) and 18.8±3.7 ml/kg, respectively. These values are comparable to those previously reported [4, 5].

Shown in Fig. 2 is the transfer function from CSP to Ees in an animal. The transfer function approximates a second-order delay system with a cut-off frequency of 0.023 Hz. These finding are consistent with that reported [2].

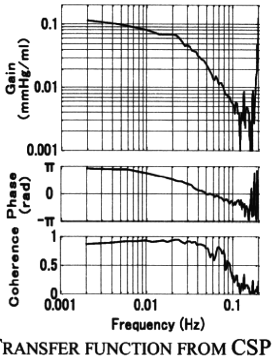

FIG. 2. TRANSFER FUNCTION FROM CSP TO Ees

Illustrated in Fig. 3 are the time series of CSP, predicted AP (solid line) and measured AP (dotted line) in an animal. The predicted AP matches reasonably well with those measred. The correlation coefficent (r2) varied between 0.80 and 0.93. The standard error of estimate ranged between 4.4 and 7.6 mmHg (3.0-7.2 % of mean AP) suggseting the reasonable accuracy of prediction.

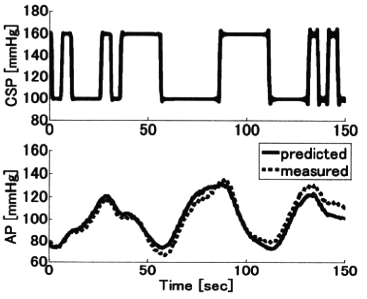

FIG. 3. PREDICTION OF THE DYNAMIC CHANGE OF AP

IV. Discussion

We have shown that the framework of circulatory equilibrium, which is an extension of the classic Guyton's framework, could predict the changes of AP induced by baroreflexly modulated ventricular and vascular properties.

The extended Guyton's framework developed by the authors' group has been shown to accurately represent the circulatory equilibrium under steady state conditions [4, 5]. However, whether the model holds under dynamic conditions remained unanswered. Furthermore, in the present study, we predicted the dynamic baroreflex induced responses of Ees, HR, R and V with a set of linear transfer functions. Since the baroreflex system is known to be nonlinear, how the nonlinearity in the baroreflex system impacts the accuracy of predictions remained unknown. The results of present study indicated that we could linearly predict baroreflexly modulated ventricular and vascular properties reasonably well and the framework of circulatory equilibrium holds under the condition where baroreflex dynamically changes arterial pressure.

V. Conclusion

We conclude that the proposed framework of circulatory equilibrium holds under baroreflex induced dynamic changes in hemodynamic conditions.

Acknowledgment

This study was supported in part by Health and Labour Sciences Research Grant for Research on Medical Devices for Improving Impaired QOL from the Ministry of Health Labour and Welfare of Japan, Health and Labour Sciences Research Grant for Clinical Research from the Ministry of Health Labour and Welfare of Japan, and Grant-in-Aid for Scientific Research(S) (18100006) from the Japan Society for the Promotion of Science.

References

[1] A.C. Guyton, and John E. Hall, "Textbook of Medical Physiology, eleventh edition", *pp. 230-231. 2006.*

[2] T. Kubota, J. A. Alexander Jr, R. Itaya, K. Todaka, M. Sugimachi, K. Sunagawa, Y. Nose and A. Takeshita, "Dynamic effects of carotid